EFFECT OFWIND SPEED ON THE CRITICAL WIDTH OF SIMULATION REGION FOR THE DRAG TYPE VAWT

M. ZHENG, L. ZHANG

Institute for Energy Transmission Technology and Application, School of Chemical Engineering,
Northwest University, Xi'an 710069, China
mszheng2@yahoo.com

Abstract - In the present paper, the effect of wind speed on the critical width of simulation region for the 5- blade drag typed VAWT is studied, which is based on simulation of CFD with FLUENT soft. Sliding grid and PISO algorithm are employed in the simulation. Varying inlet wind speeds from 6.0m/s to 9.0m/s, are employed to perform the effect of wind speed study. It indicated that the critical width of the simulated region increases with the inlet wind speed linearly.

Keywords: simulation; critical width; simulation region; drag type VAWT; wind speed.

1. INTRODUCTION

The progress of human civilization consumes a large amount of energy with the development of science & technology. Actually, the resource of fossil fuel is limited. The massive exploitation of fossil fuel will lead to an energy crisis gradually and it in turn restricts the development of science and technology and social progress [1].

In nowadays, the increasing exploitation and use of fossil fuels result in serious environmental problems, such as hole in the ozone layer, sea levels rising, and acid rain, etc. Therefore, the development and application of renewable and clean energy have become an inevitable choice so as to replace traditional energy sources in the future.

Renewable clean energy exhibits a bright potential in the future [2-4]. Wind energy is one of the inexhaustible renewable energy, which distributes widely and almost everywhere without pollution [1]. Therefore, it received more interests these years.

1.1. Status of wind turbine research and application

Wind turbine is the basic element of wind power machinery. Two basic kinds of wind turbine have been developed in general [5], i.e., vertical axis wind turbines (VAWT) and horizontal axis wind turbine (HAWT). According to the property of the force acting on the blade, wind turbine can be further divided into drag type and lift type.

The VAWT occupies a large share of the market in small wind turbine region. Also, the character of low speed of VAWT results in much smaller noise under working condition. As to this perspective, it is more convenient for ordinary people to use VAWT instead of HAWT.

In summary, it can be seen that the VAWT has some advantages such as low noise, omni-direction, easy starting and installation, simple structure, etc, it can be used in some special regions [6,7].

1.2. CFD and the numerical simulation of wind turbine

1.2.1. Application status of fluid mechanics calculation method

Computational Fluid Dynamics (CFD) is an effective method to simulate the behavior of fluids; it has been widely used in the design and research of machine and production process in nowadays.

Although CFD was proposed early in 1970s, its development is rather slow due to the low level of computer hardware technology at that time. Until 1990s, the rapid development of computer hardware promotes the progress of CFD gradually, which also improves the computation technology and its precision greatly. Currently, the application of CFD technology has covered almost all fields of human production and living, and forms a variety of commercial CFD software, such as FLUENT, CFX, Star - cd, Phoenics, etc. Table 1 shows the typical applications of CFD.

Table 1. Typical application fields of CFD

Field	Purpose	Applicable places
Automobile industry	Improve the performance of modern cars	Automobile flow around; Combustion and flow process in engine; Indoor air condition
Manufacturing	Understand the characteristics of liquid metal flow	Simulation the process of the iron and steel smelting
Oil industry	Simulate working conditions; Improve equipment	Use special tools for oil water separation
Shipbuilding industry	Deal with hydrodynamics problem	Solve problems such as submarines and torpedoes

1.2.2. The application of CFD in wind energy field

With the rapid development of computer technology, CFD obtains rapid progress, it appeared more numerical simulation method such as time average method (RANS), direct numerical simulation and large eddy simulation. The RANS has mature turbulence model, such as Baldwin - Lomax model, Spalart- Allmaras model and k-ε model. At the same time, some other general fluid calculation software is also available in the market, such as Fluent, CFX and STAR-CD. CFD has been employed to calculate the unsteady flow accurately and quickly. CFD method is more general and intuitive as compared with the stream-tube method and vortex method. As to CFD, the flow field around the wind turbine's rotor could be captured accurately; velocity field and pressure field around the rotor could be displayed visually through the visualization technology, so that the aerodynamic performance of rotor could be analyzed accurately.

Naccache G. and Paraschivoiu M. conducted parametric study of the dual vertical axis wind turbine using CFD [8]; Verkinderen E. and Imam B. Aproposed a simplified dynamic model for mast design of H-Darrieus vertical axis wind turbines (VAWTs) [9]; Shaaban S., Albatal A. and Mohamed M.H. conducted optimization of H- Rotor Darrieus turbines' mutual interaction in staggered arrangements [10]. Talukdar P. K., Sardar A., and Kulkarni V., et al. Performed Parametric analysis of model Savonius hydrokinetic turbines through experimental and computational investigations [11]. In Ref. [12], the length effect of simulation region on simulation results is studied fundamentally. It indicated that the relative standard error of the outline wind speed with respect to that of the infinite position could be less than 5% under condition of the simulation scale length longer than 140m for a 5-blade VAWT, for the rotor with radius and the blade of 2.0m and 0.76m, respectively. The effect of blade angle of the 5-blade VAWT on efficiency was studied in Ref. [13], the maximum efficiency 28.48% is obtained at the blade angle 19° for the turbine with the rotor's radius 2.0m and the optimized blade width 0.78m at rotation rate 17 rpm s and wind speed of 8 m/.

Through the overall analysis of the status of application of CFD in wind turbine study, it can be seen that the most simulation by using CFD to analyze windmill features is conducted in the region of 3 to 5 times of the diameter of windmills as the simulation scale up to now, and the discussion concerning the influence of size of calculation region on the calculation results is quite rare [1,14]. However, as is known that the size of calculation region has inevitably significant effect on the calculation result, this kind of study is worth to be done in detail.

In this paper, CFD is employed as a research method, and combined with the general fluid mechanics calculation software FLUENT, to perform a numerical simulation for the 5-blade drag-type VAWT, so as to investigate the influence of the width of calculation region on the simulation results.

2. MATHMATICAL EQUATIONS DSCRIBING THE FLOW PROPERTY OF WIND FIELD

According to the geometric and operating features of straight blade of VAWT, the flow field of each cross-section along the blade height direction is almost the same, the flow velocity along the blade height direction is approximately zero, therefore the simulation can be simplified to a 2-D flow field one so that the amount of calculation could be reduced, and k-ω SST turbulence model is employed. The controlling equations is

$$\frac{\partial(\rho k)}{\partial t} + \frac{\partial(\rho k u_i)}{\partial x_i} = \frac{\partial(\Gamma_k \frac{\partial k}{\partial x_j})}{\partial x_j} + \tilde{G}_k - Y_k + S_k \qquad (1)$$

$$\frac{\partial(\rho \omega)}{\partial t} + \frac{\partial(\rho \omega u_i)}{\partial x_i} = \frac{\partial(\Gamma_\omega \frac{\partial \omega}{\partial x_j})}{\partial x_j} + G_\omega - Y_\omega + D_\omega + S_\omega \qquad (2)$$

in which, k is the turbulent kinetic energy; ω stands for dissipation rate; u shows the velocity component; ρ indicates the fluid density; t is time; x is coordinate; Γ_k and Γ_ω for diffusion; G_k and G_ω for turbulent momentum terms; Y_k and Y_ω turbulent loss of k and ω, D_ω represents the cross diffusion, S_k and S_ω for source terms defined by user. The specific equation for each term is listed in Eqs. (3) - (9),

$$\tilde{G}_k = \min(-\rho \overline{u'_i u'_j} \frac{\partial u_j}{\partial x_i}, 10\rho \beta^* k\omega) \qquad (3)$$

$$G_\omega = -\rho \overline{u'_i u'_j} \frac{\partial u_j}{\partial x_i} \alpha \frac{\omega}{k} \qquad (4)$$

$$\Gamma_k = \mu + \frac{\mu_t}{\sigma_k} \qquad (5)$$

$$\Gamma_\omega = \mu + \frac{\mu_t}{\sigma_\omega} \qquad (6)$$

$$Y_k = \rho \beta^* k\omega \qquad (7)$$

$$Y_\omega = \rho \beta \omega^2 \qquad (8)$$

$$D_\omega = 2(1 - F_1)\rho \frac{1}{0.856\omega} \frac{\partial k}{\partial x_j} \frac{\partial \omega}{\partial x_j} \qquad (9)$$

in which, σ_k and σ_ω are turbulent Prandtl number of k and ω, respectively; μ_t is viscosity of fluid, μ_I is the turbulent viscosity coefficient, u_i' is the fluctuating velocity component, respectively. The specific equation for each term is represented as,

$$\sigma_k = \frac{1}{F_1/0.85 + (1-F_1)/1} \qquad (10)$$

$$\sigma_\omega = \frac{1}{F_1/0.5 + (1-F_1)/0.856} \qquad (11)$$

$$\mu_t = \frac{\rho k}{\omega} \frac{1}{\max[\frac{1}{\alpha^*}, \frac{9SF_2}{5\omega}]} \qquad (12)$$

$$\alpha^* = \alpha_\infty^* \left(\frac{0.024 + \rho k/6\mu\omega}{1 + \rho k/6\mu\omega} \right) \qquad (13)$$

$$\alpha = \frac{0.52}{\alpha^*} \left(\frac{1/9 + \rho k/2.95\mu\omega}{1 + \rho k/2.95\mu\omega} \right) \qquad (14)$$

$$F_1 = \tanh(\phi_1^4) \qquad (15)$$

$$\phi_1 = \min\left[\max\left(\frac{\sqrt{k}}{0.09\omega y}, \frac{500\mu}{\rho y^2 \omega} \right), \frac{4\rho k}{\sigma_{\omega,2} D_\omega^+ y^2} \right] \qquad (16)$$

$$D_\omega^+ = \max\left[2\rho \frac{1}{\sigma_{\omega,2}} \frac{1}{\omega} \frac{\partial k}{\partial x_j} \frac{\partial \omega}{\partial x_j}, 10^{-10} \right] \qquad (17)$$

$$F_2 = \tanh(\phi_2^2) \qquad (18)$$

$$\phi_2 = \max\left[2\frac{\sqrt{k}}{0.09\omega y}, \frac{500\mu}{\rho y^2 \omega} \right] \qquad (19)$$

$$\beta^* = \beta_i^* [1 + 1.5F(M_t)] \qquad (20)$$

$$\beta_i^* = 0.09 \left(\frac{4/15 + (\rho k/8\mu\omega)^4}{1 + (\rho k/8\mu\omega)^4} \right) \qquad (21)$$

$$\beta = 0.072 \left[1 - \frac{1.5\beta_i^*}{0.072} F(M_t) \right] \qquad (22)$$

$$F(M_t) = \begin{cases} 0 & M_t \le M_{t0} \\ M_t^2 - M_{t0} & M_t > M_{t0} \end{cases} \qquad (23)$$

$$M_t^2 \equiv \frac{2k}{\gamma RT} \qquad M_{to} = 0.25 \qquad (24)$$

3. SIMULATIONS

Transient calculation is adopt for 5-blade drag type VAWT, which differs from SIMPLE algorithm. PISO algorithm is based on the basic variables of pressure, it is a kind of time division algorithm [12,13]. A multi - step correction in each time step in the transient calculation is involved in PISO algorithm, which is employed to ensure the computational efficiency and the precision of transient

calculation. In order to ensure to the accuracy of the numerical calculations, turbulence model k-ω SST is chosen to conduct the simulation.

3.1 The geometric modeling and mesh of 5-blade drag-type VAWT

The real flow field around wind turbine is a 3 dimensional one, but the flow field at each cross section of the blade height is basically the same except at the blade ends. So, 2- dimensional simulation is frequently employed to perform the calculation [12,13]. A 2-D computation model is shown in Fig. 1. The whole flow field are divided into three zones in Fig. 1, says Z_1, Z_2, and Z_3. In Fig. 1, the central circular zone is named by Z_3 with radius of 1 m, in which a stationary flow field runs; the annular sliding zone with the outer radius of 2.2 m is named Z_2, 5 blades is included here; the rectangular area is named as Z_1, which is excluded zones Z_1 and Z_2. H and L indicate the width and the length of the whole computation region, respectively. While, the inlet wind speed and rotational rate of the turbine are expressed by V and ω, respectively.

The wind turbine is with following geometric size, the blade is a semicircle with the radius of is 0.4m, the wind turbine rotor is with the radius of 2 m. A grid-independence model is used to conduct the computation. The quadrilateral cells is chosen for mesh; finer mesh is made near the rotor and rougher mesh is made for positions far from the rotor. Finally, 2.6×10^5 cells is reached for the total number of the grid. The the stationary zone and sliding zone are separated by an interface, which is superposed by the two interfaces [12,13].
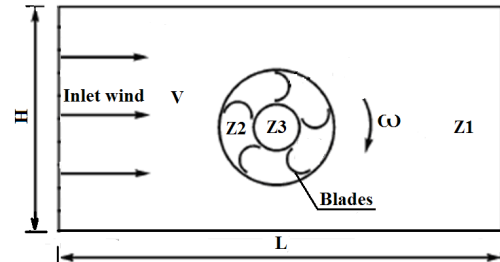

**Fig.1. Schematic diagram of geometric sliding domain and calculation region**

In the light of [12,13], the rectangular calculation region is with the size of 70 m×140 m firstly. The inlet wind is from the left bound of the calculation region with the speed of V. The turbine center is 20m far from the inlet line of the calculation region backward.

Borders are set for each zone, while the borders of the two concentric circles are actually overlapped. The calculating data on the overlapped borders is needed to exchange during calculations. Adequately, the number of node around wind blade increases. Table 2 shows the number of nodes on the each line.

Table 2. Number of nodes on the each line

| Line	Number of node
On each edge of width H	196
On each edge of length L	392
Overlapping circle between Z_1 and Z_2	420
Overlapping circle between Z_2 and Z_3	210
Each semicircle blade	80

The grid "quad" and "pave" are set as long as the node setting is performed. Eventually, Figs. 2 and 3 show the global grid and the detailed grid around blade. Table 3 is the situation of mesh generation for each zone.
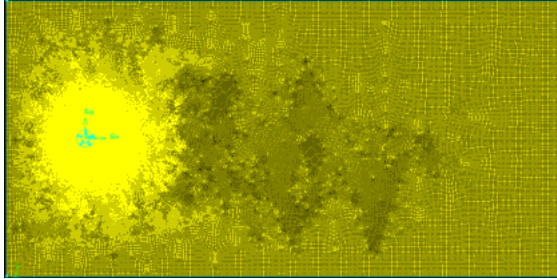
Fig. 2. Global Grid
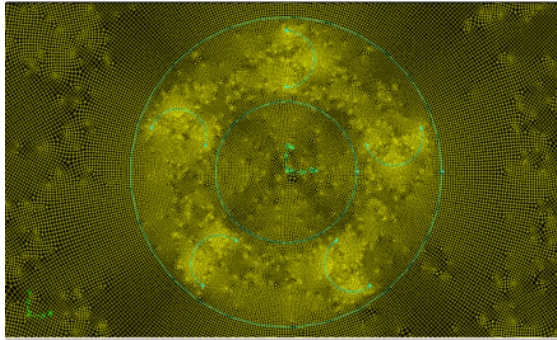
(1) Graph for partial grid
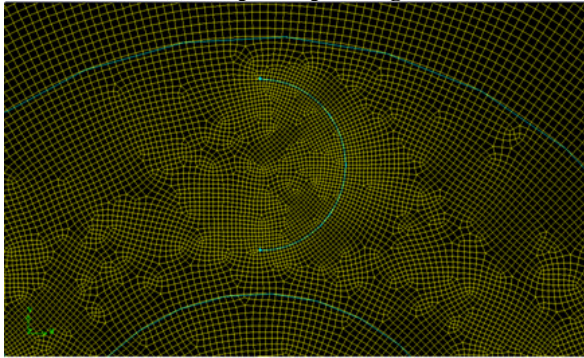
(2) Enlarged graph for grid

Fig. 3. Grid details around blade

Table 3. Mesh generation for each zone

Zone	Number of grid
Z_1	236562
Z_2	23316
Z_3	3877
Total	263755

3.2. Boundary conditions and solvers setting
3.2.1. Boundary conditions

The boundary condition is selected as "velocity inlet" for the inlet boundary; the outlet boundary condition is set as free flow (outflow); initially symmetrical boundary condition is employed for both sides of the long border (symmetry); "wall" is set for the surface of the blade, within Z_2 region blades move together with the sliding zone, which is with the relative speed 0; "interfacial boundary" is set for interface between zones.

3.2.2. The solvers setting

The modeling of drag type 5-blade VATW is transient calculation, pressure -based is used as the choice of the solving method in FLUENT. PISO algorithm is employed for the numerical algorithm of control equations. 0.02s is selected as the time step, and calculation is conducted till 4000 steps, the total time for every simulation working is 80s. At the end of each time step, the moment coefficient (Cm) is output.

3.2.3 Calculation for moment and power efficiency

The moment coefficient Cm varies with time. As is shown Fig. 4, the variation of moment coefficient Cm is conducted by using FLUENT software as data processing function. The size of rectangular region 70 m×140 m is employed for the calculation. The inlet wind speed is 8 m/s, and the rotational rate of the rotor is 17rpm for a 1 m height 5-blade wind turbine.

It could be seen from Fig. 4 that the moment coefficient is with period of about 7s. On the other hand, it could obtain an averaged value for moment coefficient Cm_A in several periods. Furthermore, the power of the wind turbine P could be obtained from Eq. (25),

$$P = C_{mA} \cdot C \cdot \omega/60. \tag{25}$$

While, the power efficiency is

$$\eta = P/(\rho \cdot V^3 \cdot h \cdot D/2) \tag{26}$$

in which, $C=0.6125$ is a factor; ρ is density of air; ω is the rotational rate of the rotor (rad/min); V is wind speed; D is diameter of the wind turbine; h is the height of the wind turbine. The term $\rho V^3 hD/2$ expresses the power of the inlet wind.

For the wind turbine with height of 1 m, it obtains the averaged torque 179.59 N·m from Fig. 4 at inlet wind speed of 8 m/s and rotational speed 17 rpm for a drag-type 5-blade VAWT. The corresponding power of this rotor is 313.31 W. While, the efficiency of this turbine is 24.98%.
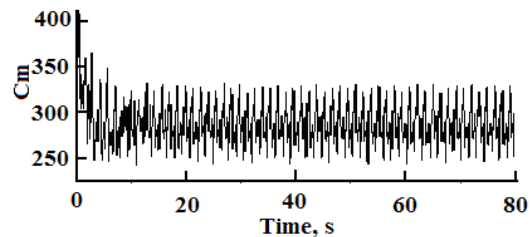
Fig. 4. The moment coefficient Cm vs time (0-80s)

3.3. Size effect of simulation region

In principle, the simulation region is as bigger as possible. However, big simulation region induces more grid number, and more space and time. Therefore, the size designation for a simulated calculation is a very important, which influences the calculation results significantly.

3.3.1. Size and grid designation for the 5-blade VAWT

In [12], it discussed the effect of length of the simulated calculation region on the results, it obtained a conclusion that for a 5-blade VAWT with rotor radius of 2m, the length of the calculating region should be longer than 140 m, so as to keep the relative standard error of wind speeds at the exit of region less than 5% as compared with those at the infinite position.

However, there is no report on the effect of width of the calculation region on the calculation results.

In this section, the influence of the width of calculation region on calculation result is discussed. The simulation is carried out by varying the width of the calculation region while designating the length of the calculation region as 140m, the inlet wind speed and the rotational rate are fixed as 8m/s and 17rpm, respectively. The designated widths of the simulation region are listed in Table 4.

In order to make the above 5 cases mutually comparable, the grid number needs to increase with the width correspondingly. As a result, the grid number in Z_1 increases at the same partition density, while grid number keeps invariable in zone Z_2 and Z_3. Finally, it got the grid number for the 5 cases, as shown in Table 5.

Table 4. Parameters for simulation under varying widths condition

Case no.	1	2	3
The width of the region (m)	60	65	70
The length of the region (m)	140	140	140
The distance from inlet boundary to wind turbine center (m)	20	20	20
Case no.	4	5	
The width of the region (m)	75	80	
The length of the region (m)	140	140	
The distance from inlet boundary to wind turbine center (m)	20	20	

Table 5. The grid number of the 5 varying widths condition

Size of areas	60m×140m	65m×140m	70m×140m
Grid number in Z_3	3877	3877	3877
Grid number in Z_2	23771	23771	23771
Grid number in Z_1	232270	243144	246562
Size of areas	75m×140m	80m×140m	
Grid number in Z_3	3877	3877	
Grid number in Z_2	23771	23771	
Grid number in Z_1	248885	254024	

3.3.2. Error analysis

Error analysis method is used, FLUENT software is employed to get the velocity field, as well as the velocity on outline boundary of each point of the every calculation region. Eq. (27) is used evaluate the relative error analysis.

$$\delta = \frac{1}{V_0} \sqrt{\sum_{i=1}^{n} (V_0 - V_i)^2 \Big/ n} \qquad (27)$$

in which δ is relative standard errors, *n is* number of data, and V_0 is the wind speed of inlet and infinite locations.

For given inlet wind speed V_0, it obtains the wind speed value for each point on the outline boundary V_i for each width of calculation region.

3.3.2.1. Error analysis for rotation rate 17 rpm and inlet wind speed 8m/s

For the wind turbine's rotation rate 17 rpm and inlet wind speed 8m/s, it obtained the relative standard error for each width of calculation region with the help of Eq.(27), the result is shown in Fig. 5. It could be seen from the Fig. 5 that the relative standard error decreases with the increase of the width of the calculation region. This is due to the fact that the wind speed at the outline will be closer to that of the infinite position as the width of the calculation region increasing.
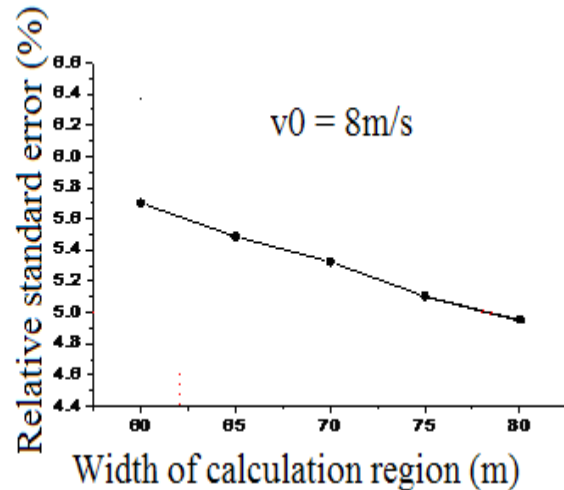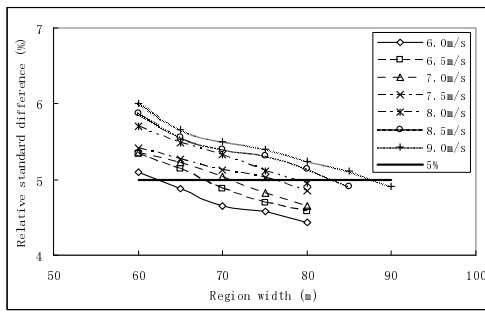

Fig.5. The relative standard errors vs region width for VAWT at v_0 = 8m/s & rotation rate 17 rpm

3.3.2.2 Error analysis for rotation rate 17 rpm and varying inlet wind speed

Take other wind speed from v_0=6m/s to 9.0m/s as the inlet values on the inlet boundary, for the wind turbine's rotation rate 17 rpm, similar results are obtained, as is shown in Fig.6.

From Fig.6, it obtains that the relative standard error increases with the increase of wind speed.

Fig.6. The relative standard errors vs region width for VAWT at various inlet wind speed & rotation rate 17 rpm

Furthermore, if we set a horizontal line at 5%, it intersects each relative standard error curves at 5% for the different wind speed, thus a critical region width is obtained from the intersected point for each inlet wind speed, and the results are shown in Table 6. It can be seen that the critical width of calculation region increases with the wind speed.

**Table 6. Critical value of region width with respect to wind speed**

Wind speed (m/s)	6.0	6.5	7.0	7.5
Critical width (m)	62.0	67.7	70.8	75.6
Wind speed (m/s)	8.0	8.5	9.0	
Critical width (m)	78.5	83.1	87.6	

The data in Table 6 is drawn into Fig. 7, it gets a linear correlation between the critical width and the inlet wind speed under the condition of the relative error of outlet boundary wind speed of 5% with respect to the infinite wind speed.

The approximate relationship between critical width area and the inlet velocity is,

$$y = 8.264v_0 + 13.032 \qquad (28)$$

in which, y is the critical width of calculation area, m; v_0 is the velocity of inlet wind speed, m/s.
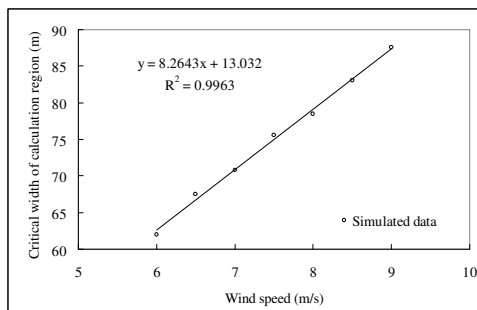
Fig.7. Variation of critical region width with respect to wind speed at relative standard error 5%

4. CONCLUSION

In conclusion, it is concluded that the critical width of the simulation region increases with the wind speed if the relative standard error of the outline speed 5% is set as the limitation for the inlet wind speeds from $v_0 = 6$ m/s to 9.0 m/s. The critical width of calculation region increases linearly with the wind speed in the calculated scopes, the approximated relationship between the critical width of calculation region and the inlet velocity is: $y = 8.264v_0 + 13.032$.

• **Statement**: none of the authors have any competing interests in the manuscript.

REFERENCES

[1] Zheng M., Guo L., Li Y., Tian Y., Teng H. P., Hu J., Zhao Y., Yu L. J. Power Efficiency of 5 Blade Drag Type Vertical Axis Wind Turbine, Applied Solar Energy, 2015; 51(3): 225–231.

[2] Zakhidov R. A., Lutpullayev S. L. Global Trends in Alternative Energies and Problems in Uzbekistan for the Development of Renewable Energy Sources, Applied Solar Energy, 2015; 51(1): 50–61.

[3] Tadjiev U. A., Kiseleva E. I., Tadjiev M. U., Zakhidov R. A. Potential of Improving Energy Efficiency of the Andijan HEPP Making Use of Wind Farms: Part II, Applied Solar Energy, 2013; 49(3): 158–164.

[4] Tadjiev U. A., Kiseleva E. I., Tadjiev M. U., Zakhidov R. A. Opportunities of Increase of Energy Efficiency of Andijan Hydro Power Plant Using Wind Farms. Part 1, Applied Solar Energy, 2014; 50(3): 171–177.

[5] Jiang C., Yan Q. Comparative Study between Horizontal axis and Vertical Axis Wind Turbines, Shanghai Electric Power. 2007; 20(2): 163- 165.

[6] Qamar S. B., Janajreh I. Investigation of Effect of Cambered Blades on Darrieus VAWTs, Energy Procedia, 2017, 105, 537-543.

[7] Abdalrahman G., Melek W., Lien F. Pitch Angle Control for a Small-scale Darrieus Vertical Axis Wind Turbine with Straight Blades (H-Type VAWT), Renewable Energy, 2017, 114, Part B, 1353-1362.

[8] Naccache G., Paraschivoiu M. Parametric study of the dual vertical axis wind turbine using CFD, Journal of Wind Engineering & Industrial Aerodynamics, 2018, 172, 244–255

[9] Verkinderen E., Imam B. A simplified dynamic model for mast design of H-Darrieus vertical axis wind turbines (VAWTs), Eng. Struct., 2015, 100, 564-576.

[10] Shaaban S., Albatal A., Mohamed M.H. Optimiza-tion of H-Rotor Darrieus turbines' mutual interaction in staggered arrangements, Renewable Energy, 2018, 125, 87-99.

[11] Talukdar P. K., Sardar A., Kulkarni V., et al. Parametric analysis of model Savonius hydrokinetic turbines through experimental and computational investigations, Energy Conversion and Management, 2018, 158, 36-49.

[12] Li Y., Zheng M., Teng T., Hu J. Numerical Simulation of 5 - blade Resistance Type Vertical Axis Wind Turbines, Chemical Eng. (China). 2014; 42(8): 51-55.

[13] Zheng M, Li Y., Tian Y., et al Effect of Blade Installation Angle on Power Efficiency of Resistance Type VAWT by CFD study, International Journal of Energy and Environmental Engineering. 2014; 6(1): 1-7.

[14] Yao Y.X., Tang Z.P., Wang X.W. Design Based on a Parametric Analysis of a Drag Driven VAWT with a Tower Cowling, J. Wind Eng. Ind. Aerodyn. 2013; (116) 32–39.